Secreted chemokines reveal diverse inflammatory and degenerative processes in the intervertebral disc of the STZ-HFD mouse model of Type 2 diabetes

Christian E. Gonzalez[1], Rachana S. Vaidya[4], Sade W. Clayton[4], Simon Y. Tang[1-4]

[1]Department of Biomedical Engineering, Washington University in St. Louis, St. Louis, MO
[2]Institute of Material Science and Engineering, Washington University in St. Louis, St. Louis, MO
[3]Department of Mechanical Engineering and Materials Science, Washington University in St. Louis, St. Louis, MO
[4]Department of Orthopaedic Surgery, Washington University School of Medicine, St. Louis, MO

Corresponding Author:
Simon Y. Tang, Ph.D., MSCI
Associate Professor
Orthopedic Surgery, Biomedical Engineering,
Mechanical Engineering & Materials Science
Washington University in St. Louis
simon.tang@wustl.edu

Keywords: type 2 diabetes; intervertebral disc degeneration; streptozotocin-high-fat-diet; leptin receptor deficiency; chronic inflammatory cytokines

Abstract

The chronic inflammation present in type 2 diabetes causes many chronic inflammatory comorbidities, including cardiovascular, renal, and neuropathic complications. Type 2 diabetes is also associated with a number of spinal pathologies, including intervertebral disc (IVD) degeneration and chronic neck and back pain. Although confounding factors such as obesity are thought to increase the loads to the musculoskeletal system and subsequent degeneration, studies have shown that even after adjusting age, body mass index, and genetics (e.g. twins), patients with diabetes suffer from disproportionately more IVD degeneration and back pain. Yet the tissue-specific responses of the IVD during diabetes remains relatively unknown. We hypothesize that chronic diabetes fosters a proinflammatory microenvironment within the IVD that accelerates degeneration and increases susceptibility to painful disorders. To test this hypothesis, we evaluated two commonly used mouse models of diabetes – the leptin-receptor deficient mouse (db/db) and the chronic high-fat diet in mice with impaired beta-cell function (STZ-HFD). The db/db is a genetic model that spontaneous develop diabetes through hyperphagia, while the STZ-HFD mouse first exhibits rapid obesity development under HFD and pronounced insulin resistance following streptozotocin administration. Both animal models were allowed to develop sustained diabetes for at least twelve weeks, as defined by elevated hemoglobin A1C, hyperglycemia, and glucose intolerance. Following the twelve-week period, the IVDs were extracted in quantified in several measures including tissue-specific secreted cytokines, viscoelastic mechanical behavior, structural composition, and histopathologic degeneration. Although there were no differences in mechanical function or the overall structure of the IVD, the STZ-HFD IVDs were more degenerated. More notably, the STZ-HFD model shows a significantly higher fold increase for eight cytokines: CXCL2, CCL2, CCL3, CCL4, CCL12 (monocyte/macrophage associated), IL-2, CXCL9 (T-cell associated), and CCL5 (pleiotropic). Correlative network analyses revealed that the expression of cytokines differentially regulated between the db/db and the STZ-HFD models. Moreover, the STZ-HFD contained a fragmented and modular cytokine network, indicating greater complexities in the regulatory network. Taken together, the STZ-HFD model of type 2 diabetes may better recapitulate the complexities of the chronic inflammatory processes in the IVD during diabetes.

Introduction

{Figure 1}

Type 2 diabetes (T2D) is a prevalent metabolic disorder marked by insulin resistance and prolonged hyperglycemia, impacting millions around the globe and leading to significant healthcare expenses (Srinivasan and Ramarao, 2007; Boucher et al., 2014; Petersen and Shulman, 2018; United States, Center for Disease Control, 2022). This disease shares several characteristics with autoimmune disorders, including the chronic, systemic overexpression of immunomodulating cytokines, which can gradually lead to widespread accrual of tissue damage across multiple organ systems (Itariu and Stulnig, 2014; Chen et al., 2017; de Candia et al., 2019; Daryabor et al., 2020). Intervertebral disc (IVD) degeneration is a comorbidity of particular interest due to strong evidence for chronic-inflammatory etiology (Risbud and Shapiro, 2014; Molinos et al., 2015; Navone et al., 2017; Lyu et al., 2021; Pinto et al., 2023) and low back pain is a potently association with chronic T2D (Robinson et al., 1998; Jhawar et al., 2006; Sakellaridis, 2006; Liu et al., 2018; Alpantaki et al., 2019; Cannata et al., 2019; Broz et al., 2021). In T2D, chronic inflammation driven by a persistent milieu of chemokines may foster a pro-degenerative microenvironment within the IVD, potentially linking T2D-induced inflammation to accelerated IVD degeneration.

Various animal models are used to study T2D, primarily being rodent models due to their cost-effectiveness, ease of handling, and genetic similarities to humans. Models can be classified into genetic (spontaneously induced) and non-genetic (experimentally induced) types. Typical genetic models involve animal strains with inherent mutations predisposing the animal to developing T2D, while experimentally-induced models typically employ some combination of chemical induction, dietary manipulations, and surgical methods (Srinivasan and Ramarao, 2007; Islam and Wilson, 2012). Each model mimics different aspects of T2D pathogenesis, such as insulin resistance and beta-cell dysfunction, but none can entirely replicate the human condition. The $Lepr^{db}$ (db/db) mouse, a particularly popular model for studying T2D, is characterized by a point mutation in the *db* gene, leading to the inactivation of the leptin receptor [**Fig. 1A**] (Chen et al., 1996; Lee et al., 1996). This model exhibits metabolic characteristics similar to human T2D, including severe obesity, hyperglycemia, insulin resistance, and hyperinsulinemia, making it a valuable model for studying T2D (Wang et al., 2014). The etiology of T2D in db/db mice differs from human T2D,

though, as it is driven by leptin receptor deficiency rather than a combination of genetic and lifestyle factors commonly seen in humans. This distinction complicates the direct translation of findings from this model to human T2D (Wang et al., 2014).

The db/db mouse model has been widely employed in spine research to further investigate the consequences of T2D on spinal complications. Studies focusing on the IVDs of db/db mice have shown that these mice exhibit signs of disc degeneration, including increased cell apoptosis and extracellular matrix degradation (Li et al., 2020; Natelson et al., 2020; Lintz et al., 2022). These findings suggest that the db/db model can be useful for studying T2D-induced IVD degeneration. However, the absence of functional leptin signaling complicates interpretations of these changes as it may independently affect IVD homeostasis. Leptin, beyond its well-known role in energy regulation and appetite control, influences various systemic functions, including immune response modulation, bone formation, and reproductive health (Francisco et al., 2018). In the musculoskeletal system, leptin affects chondrocyte proliferation, osteoblast activity, the synthesis of extracellular matrix proteins, and many more tissue- and cell-level functions crucial for maintaining homeostasis (Gruber et al., 2007; Li et al., 2013; Han et al., 2018; Sharma, 2018; Segar et al., 2019; Curic, 2021). Leptin's responsibilities in the IVD specifically include promoting anabolic processes and reducing catabolic activities, thereby supporting disc health (Li et al., 2013; Han et al., 2018). Consequently, the lack of leptin signaling in db/db mice might mask or alter the degenerative pathways activated by the diabetic condition, potentially confounding observations of the diabetic milieu with those of leptin ablation. This complicates the interpretation of T2D-related changes in the IVD observed in this model, as the effects could be due to the absence of leptin signaling rather than diabetes alone.

In contrast, the Streptozotocin-High Fat Diet (STZ-HFD) model offers a non-genic approach to replicating T2D. It induces the condition through pro-glycemic diet and low-dose streptozotocin-induced pancreatic beta-cell dysfunction, avoiding genetic ablation of hormonal pathways like leptin (as seen in the db/db model) [**Fig. 1A**]. This model is characterized by significant metabolic disturbances to glycemic status, insulin resistance, and body weight, mirroring the human T2D phenotype more closely (Kusakabe et al., 2009; Islam and Wilson, 2012). Additional metabolic characteristics reported in STZ-HFD mouse studies include elevated serum insulin levels, dyslipidemia (increased triglycerides, LDL cholesterol, and

total cholesterol), and increased markers of inflammation and oxidative stress (Gilbert et al., 2011; Alquier and Poitout, 2018; Yin et al., 2020). This sets this mouse model apart as valuable tool for studying the complex interactions within diabetic complications without the confounding factor of complete leptin signaling ablation (Kusakabe et al., 2009). Previously this model has been employed in studying diabetic complications in bone (Eckhardt et al., 2020). Our study aims to uncover the mechanisms behind inflammatory-pathway contribution to IVD degeneration and dysfunction, advancing the field's understanding of T2D-related IVD complications.

Inflammatory cytokines are central to the pathophysiology of both IVD degeneration and T2D. They not only mediate acute inflammatory responses but also perpetuate chronic inflammation, leading to tissue degradation (Guest et al., 2008; Velikova et al., 2021). Key proteins such as ADAMTs and MMPs, regulated by cytokines, are instrumental in the degradation of extracellular matrix in the IVD, furthering degeneration (Bond et al., 1998; Malemud, 2019). The identification and characterization of these cytokines in the context of T2D can elucidate potential therapeutic targets and markers for early intervention (Al-Shukaili et al., 2013; Herder et al., 2013).

Studies have shown that inflammatory cytokines are involved in the degradation of IVD tissue, contributing to conditions like pain and disc degeneration (Shamji et al., 2010; Risbud and Shapiro, 2014). Research indicates that pro-inflammatory cytokines, such as TNF-α, IL-1β, and IL-6, are upregulated in degenerated and herniated disc tissues, perpetuating the inflammatory response and leading to further tissue damage (Wuertz and Haglund, 2013; Molinos et al., 2015; Navone et al., 2017; De Geer, 2018). Moreover, these cytokines influence the expression of matrix-degrading enzymes like ADAMTS-4 and MMP-9, which are crucial for the breakdown of extracellular matrix components, exacerbating disc degeneration (Tian et al., 2013; Zhang et al., 2015).

The role of inflammatory cytokines in T2D is also well-documented. They contribute to insulin resistance and beta-cell dysfunction, key features of T2D (Calle and Fernandez, 2012). Studies have identified elevated levels of pro-inflammatory cytokines in T2D patients, suggesting their role in the disease's progression and complications (Guest et al., 2008; Velikova et al., 2021). Targeting these cytokines could provide novel therapeutic approaches for both T2D and IVD degeneration, highlighting the interconnected nature of these conditions (Al-Shukaili et al., 2013; Herder et al., 2013).

This study seeks to shift the research focus towards using the STZ-HFD model by comparing the overall IVD health between the db/db and STZ-HFD mouse models, with a particular focus on inflammation and related complications. We will examine inflammation and broad genomic changes in functional spine units to understand the molecular mechanisms at play. Additionally, degeneration and morphological changes will be assessed to determine the extent of tissue damage and structural alterations. Finally, the mechanical function of the intervertebral discs will be evaluated to understand the impact of T2D. By investigating these comprehensive metrics [**Figure 1C**], we aim to dissect the specific pathways through which T2D exacerbates IVD degeneration. Our findings will enhance the understanding of the interplay between T2D and IVD homeostasis and validate the relevance of the STZ-HFD model.

Materials & Methods

Animals. In this study, we focused on skeletally-mature (12-week-old) male C57BL/6 mice (N = 20) for their established susceptibility to Type 2 Diabetes (T2D) when exposed to a high-fat diet (HFD) and treated with streptozotocin (STZ). Previous findings have indicated that this strain, particularly males, exhibits rapid obesity development under HFD and pronounced insulin resistance following STZ administration (Luo et al., 1998; Mu et al., 2006; Mu et al., 2009). As a result of estrogen-mediated mechanisms of protection, female STZ-HFD mice are resistant to developing T2D and are thus excluded from this study (Medrikova et al., 2012; Pettersson et al., 2012; Stubbins et al., 2012). To contrast the STZ-HFD model's pathology with a well-characterized model of chronic T2D, we included a parallel cohort of 3-month-old homozygous (db/db) male $Lepr^{db}$ mutant mice with heterozygous (db/+) littermate controls (N = 18), as at this timepoint they have endured a similar duration of T2D symptoms; male mice were used to avoid confounding effects of sex-based differences. All mice were group-housed (max. 5 mice per cage) under pathogen-free conditions in standard cages; the environment was controlled with a stable temperature and a 12-hour light/dark cycle, with *ad libitum* access to food and water. All procedures were approved by the Institutional Animal Care and Use Committee (IACUC) of Washington University in St. Louis. Regular health and welfare assessments were conducted, including general monitoring of weight, food supply, and behavior.

Study Design. The study was organized into two phases: initially, mice were maintained on a HFD for four to six weeks, after which they received a one-time dose of STZ and continued on the HFD for an

additional 12 weeks. The STZ-HFD group (n = 13) was given a high-fat diet (Research Diets, Inc., D12492i, 60% kcal from fat) for the duration of the study, with the Control + Vehicle group (n = 7) receiving standard mouse chow (5053 PicoLab® Rodent Diet 20, 13% kcal from fat). At the end of the initial phase, baseline measurements of body weight and fasting blood glucose were collected. Following the first phase, STZ-HFD mice were injected intraperitoneally with 100 mg/kg Streptozotocin (MilliporeSigma) in 50 mM sodium citrate buffer (pH 4.5), with Con+Veh animals receiving the sodium citrate buffer only. The two experimental groups received their respective diets for 12 weeks following the injection (experimental phase), and animals were assessed for diabetic status via glucose tolerance. Finally, animals were euthanized, and sterile coccygeal functional spine units (FSUs) including IVDs were harvested from each animal for organ culture and terminal measurements. The overall study design is outlined in the schematic in **Fig. 1B** and **Fig. 1C**.

Measures of diabetic status. As previously mentioned, several measures of diabetic status were collected at various points throughout the experimental phase, including fasting blood glucose, % A1C, and glucose tolerance. Blood glucose levels (mg/dL) were measured using a glucometer (GLUCOCARD Vital® Blood Glucose Meter). Blood samples were drawn via superficial incision to the tail tip of fasted mice using a scalpel; the tail was immediately treated with analgesic (Kwik Stop® Styptic Powder) after blood collection. The percentage of glycated hemoglobin (% A1C) was measured using the A1CNow®+ system (PTS Diagnostics) according to kit instructions. Blood samples were drawn in the same way as during the blood glucose test. Finally, to assess glucose tolerance (oral glucose tolerance test, oGTT), mice were fasted and had their blood glucose measured as described above to establish a baseline. Mice were then injected intraperitoneally with 2 g/kg glucose in sterile water. Additional blood glucose measurements were taken at 30 min., 60 min., and 90 min. post injection. The area-under-the-curve of blood glucose (mg•h/dL) was calculated over the course of the test. For the purpose of evaluating diabetic status for inclusion in the study, a cutoff of 435 mg•h/dL on the GTT, established in previous studies on human T2D criteria (Sakaguchi et al., 2015), was adjusted for time and interspecies differences in blood glucose levels.

Organ culture. Following extraction, FSUs were cultured in 2 mL Dulbecco's Modified Eagle Medium/Nutrient Mixture F-12 Ham with L-glutamine and 15 mM HEPES (Sigma-Aldrich, D6421) .

Culture medium was supplemented with 20% fetal bovine serum (Gibco No. A5256801) and 1% penicillin-streptomycin (Gibco No. 15140122). Cultures underwent a preconditioning period of 7 days with regular media changes to account for the inflammatory response from extraction. Conditioned media was collected 48 hours after the final media change at the end of the preconditioning period and immediately frozen in -80° C.

Chemokine assay. A multiplex assay of remodeling factors and inflammatory chemokines (45-Plex Mouse Cytokine Discovery Assay, Eve Technologies Assays; CCL-2,3,4,5,11,12,17,20,21,22; CSF-1,2,3; IL-1α,1β,2,3,4,5,6,7,9,10,11,12A,12B,13,15,16,17; CXCL1,2,5,9,10; CX3CL1; IFN-γ,β1; TNFα; LIF; VEGF; EPO; TIMP-1) was performed on conditioned media samples. Cytokine levels were analyzed using Welch's t-Test. Cytokines with greater than 25% missingness across all experimental groups were excluded from further analysis. Significantly upregulated cytokines in each model were selected for a secondary fold change analysis, where protein expression levels for db/db and STZ-HFD mice were used to calculate fold change for each cytokine over the corresponding average expression of the control (db/+ and Con+Veh respectively).

Cytokine Interaction Network Construction and Analysis. To further investigate the inflammatory profiles of these T2D models, networks of cytokine interactions were constructed and analyzed using a custom MATLAB (Version: 9.13.0.2080170 R2022b) script. Networks were generated by calculating a Pearson correlation matrix for each experimental group based on cytokine expression data from the multiplex panel of conditioned media. To isolate strong protein correlations, a threshold ($|r| > 0.7$) was applied to the correlation matrices. The filtered matrices were used to create undirected graphs, with nodes representing cytokines and edges representing significant interactions. Centrality measures were calculated to determine the importance of each cytokine within the networks. Eigenvector centrality and betweenness centrality were computed for each network using the centrality function. The resulting centrality values were organized into tables and sorted to identify the top-ranking cytokines. For each centrality metric, shared high-ranking cytokines between the diabetic models and unique cytokines for each diabetic model were aggregated. Additionally, key network characteristics were extracted to understand the structure and function of the cytokine networks. The average path length was determined using the distances function to compute the shortest finite paths between all pairs of nodes. Modularity

and community structure were assessed using the Louvain community structure and modularity algorithm (Blondel et al., 2008). We also computed k-hop reachability to assess the extent to which cytokines can influence each other within one (k=1) or two (k=2) steps. The Jaccard index was used to compare the reachability matrices between different groups, providing a measure of similarity. Finally, the networks were visualized using force-directed layouts with nodes colored by eigenvector centrality and sized by betweenness centrality.

Histology. Following removal from culture, FSUs were fixed in 10% neutral-buffered formalin (Epredia™ 5735) overnight and decalcified in ImmunoCal (StatLab STL14141) for 72 hours. Samples were fixed in paraffin, sectioned in the sagittal plane at 10 µm thickness, and stained with Safranin-O/Fast Green prior to being imaged via Hamamatsu NanoZoomer with a 20x objective. Blinded histological images of the IVDs were evaluated for degeneration based on a standardized histopathological scoring system (Melgoza et al., 2021).

Contrast-enhanced Micro-computed Tomography. To prepare for imaging, functional spine units were incubated in a 175 mg/mL Ioversol solution (OptiRay 350; Guerbet, St. Louis) diluted in PBS at 37 °C. Following 4 hours of incubation, the samples underwent scanning with a Viva CT40 (Scanco Medical) at a 10-µm voxel size, using 45 kVp, 177 µA, high resolution, and a 300 ms integration time. CEµCT data was exported as a DICOM file for analysis in a custom MATLAB program (https://github.com/WashUMusculoskeletalCore/Washington-University-Musculoskeletal-Image-Analyses). After an initial Gaussian filter (kernel size = 5), functional spine units were segmented by drawing a contour around the perimeter of the IVD every 10 transverse slices and morphing using linear interpolation. This was defined as the whole disc mask. The NP was segmented from the whole disc by thresholding and performing morphological close and morphological open operations to fill interior holes and smooth NP boundaries. The volumes and intensities were calculated from the NP and whole disc regions. Disc height index (DHI) was measured by averaging the height-to-width ratio of the IVD over five slices in the mid-sagittal plane. Finally, the NP intensity/disc intensity (NI/DI) ratio and NP volume fraction (NPVF; NP volume / total volume) was computed using the intensity and volume metrics reported by the output analysis within the MATLAB program. All thresholding and analysis were performed in a blinded fashion. This approach is described in further detail in prior studies (Lin et al., 2016; Lin and Tang, 2017).

Mechanical Testing. Mechanical testing of functional spine units was performed using cyclic compression on a microindentation system (BioDent; Active Life Scientific) with a 2.39 mm probe as previously described (Liu et al., 2015). Samples were adhered to an aluminum plate and placed in a PBS bath prior to aligning the sample beneath the probe with a 0.03 N preload. Each unit was then sinusoidally loaded in compression at 1 Hz for 20 cycles with a 35 µm amplitude. A loading slope value was calculated from the linear region of the force-displacement curve, and the tan delta (loss tangent) was calculated from the phase delay between loading and displacement. This approach is described in further detail in prior studies.

Matrix Protein Assays. Whole extracted discs were used to measure the biochemical content of various matrix proteins. First, discs were digested overnight in a papain digestion buffer, after which the buffer was collected for a 1,9-dimethylmethylene blue assay of sulfated glycosaminoglycan content with a chondroitin sulfate standard (Liu et al., 2017). The disc was then subjected to high temperature bulk hydrolyzation in 12 N HCl. Hydrolysates were desiccated and reconstituted with 0.1x phosphate-buffered saline (PBS) and measured against a quinine standard for advanced glycation end product content (Liu et al., 2017). Finally, a hydroxyproline assay was used to quantify collagen content as previously described (Liu et al., 2017).

Results

{Figure 2}

The db/db and STZ-HFD Mouse Models Exhibit a Characteristically Diabetic Phenotype

Both db/db and STZ-HFD mice demonstrate hallmark features of diabetes, as evidenced by the results in **Figure 2**. Both groups exhibit AUC GTT values above the defined threshold, indicating impaired glucose tolerance [**Fig. 2A**]. The comparison between Con+Veh and STZ-HFD groups is highly significant ($p < 0.0001$), indicating particularly severe glucose intolerance in the STZ-HFD model. The terminal body weights show that db/db mice weigh significantly more than both db/+ and STZ-HFD mice, underscoring the severe obesity associated with the db/db model [**Fig. 2B**]. This highlights the db/db mice as a representative model of a more severely obese type 2 diabetic phenotype than the STZ-HFD model. The terminal fasting blood glucose levels indicate a significant difference only between the STZ-HFD and Con+Veh groups, demonstrating notable fasting hyperglycemia in the STZ-HFD model [**Fig. 2C**]. HbA1c

levels reveal no difference between db/db mice and STZ-HFD mice, but each group significantly differs from their respective controls [**Fig. 2D**]. This indicates that both models exhibit chronic hyperglycemia, confirming their relevance as models of T2D.

{Figure 3}

Histopathological Analysis Reveals IVD Degeneration in STZ-HFD Mice

The STZ-HFD models exhibited a more degenerative phenotype in a histopathological analysis of both models. **Figure 3** presents a comparison of histological phenotypes across the four groups (db/+, db/db, Con+Veh, and STZ-HFD), showing the range of histopathological scores within this study [**Fig. 3A**]. Histopathological scoring revealed that only the STZ-HFD mice exhibit significantly greater IVD degeneration compared to the control group [**Fig. 3B**]. **Figure 3C** highlights common degenerative characteristics in the IVD of STZ-HFD mice. In the Con+Veh samples, the annulus fibrosus has healthy, convexed outer lamellae (➧) and well-organized, concentric inner lamellae (▼). In contrast, the STZ-HFD samples show degenerate crimped, concave outer lamellae (⇨) and wavy, disorganized inner lamellae (▽), indicating altered matrix structure in the AF.

{Figure 4}

CT Analysis, Matrix Assays, and Mechanical Testing All Show No Major Effects in IVD Physiology

The analysis of CEμCT data, mechanical testing, and matrix protein assays revealed only one significant difference among the four groups across all nine measured outcomes. Specifically, parameters such as NI/DI, NPVF, loading slope, hysteresis energy, tan delta, and biochemical content showed no variations between groups. The only significant result was a difference in morphology between the db/db and STZ-HFD groups, as indicated by the DHI. These findings suggest that the structural integrity, mechanical behavior, and biochemical composition of the IVDs are mostly consistent across the db/db and STZ-HFD models. The lack of significant differences broadly implies that, under the conditions tested, type 2 diabetes does not markedly affect IVD properties in these models, and cannot further establish the degenerate features gleaned in the histopathological analysis. This highlights the need for more sensitive measures or longer study durations to detect subtle changes related to T2D.

{Figure 5}

Cytokines Representing a Plethora of Immune Functions Are Chronically Upregulated STZ-HFD IVDs

The comparative analysis of cytokine expression levels between db/db and STZ-HFD models provides novel insights into diabetic inflammation of the IVD. The initial comparative analysis of the two models' protein expression levels revealed that two cytokines (CCL2,3) and sixteen cytokines (CCL2,3,4,5,12; CXCL1,2,9,10; CX3CL1; IL-2,6,16; CSF-3; VEGF; LIF) were upregulated in the db/db and STZ-HFD models respectively, and thus included in the fold change analysis. In **Fig. 4A**, the fold change in cytokine levels is computed over their respective controls (db/+ for db/db, Con+Veh for STZ-HFD). The STZ-HFD model exhibited a significantly higher fold increase compared to the db/db model for 8 cytokines: CXCL2, CCL2, CCL3, CCL4, CCL12 (monocyte/macrophage associated cytokines) (Sagar et al., 2012; Arendt et al., 2013; Lança et al., 2013; Etna et al., 2014; Motwani and Gilroy, 2015; He et al., 2016; Lim et al., 2016; DeLeon-Pennell et al., 2017; Ruytinx et al., 2018; Sindhu et al., 2019; Zhang et al., 2019, 38; Huang et al., 2020; Pelisch et al., 2020; Yang et al., 2020; Xu et al., 2021a; Xu et al., 2021b; Sheng et al., 2022), IL-2, CXCL9 (T-cell associated cytokines) (Chang and Radbruch, 2007; Venetz et al., 2010; Shachar and Karin, 2013; Ochiai et al., 2015; Boff et al., 2018; Kuo et al., 2018; Mortara et al., 2018; House et al., 2020; Marcovecchio et al., 2021; Markovics et al., 2022), and CCL5 (pleiotropic cytokine) (Juhas et al., 2015; Atri et al., 2018; Kranjc et al., 2019; Chen et al., 2020; Zeng et al., 2022). **Figure 4B** shows a Venn diagram illustrating the cytokine expression profiles. The outer circle represents the STZ-HFD model, encompassing a large number of upregulated cytokines. The inner circle represents the db/db model, containing only the two upregulated cytokines, both of which are also upregulated in the STZ-HFD model. This indicates that the STZ-HFD model has a broader and more pronounced cytokine response compared to the db/db model.

{Figure 6}

Differential Network Structures Reveal Unique Inflammatory Pathways of T2D in IVD

Our analysis of cytokine networks in these two models revealed several key insights into the inflammatory pathways associated with T2D. CCL2 and CCL4 emerged as pivotal cytokines in both models based on betweenness centrality, highlighting their crucial roles in maintaining network connectivity (**Error! Reference source not found.**). In the db/db mouse model, unique cytokines were identified that are likely influenced by the absence of leptin signaling. These included CSF-3 (betweenness centrality), CXCL-5, CXCL-9, CXCL-10, and IL-4 (eigenvector centrality), and IL-11 (both

centralities) (**Error! Reference source not found.**). In contrast, the STZ-HFD mouse model, which maintains functional leptin signaling and mimics human T2D etiology, presented a different profile of unique cytokines. CXCL2 and IL-6 (betweenness centrality), and IL-16, CCL11, and CSF3 (eigenvector centrality) were central in this model (**Error! Reference source not found.**). This indicates that these cytokines may be independently regulated through pathways that are either bypassed or inhibited in the simultaneous presence of leptin signaling and T2D-associated chronic inflammation. The db/db model demonstrated a shorter average path length compared to the STZ-HFD model (**Error! Reference source not found.**), indicating more efficient communication within the cytokine network of the db/db model. The longer path length in the STZ-HFD model suggests a more dispersed network structure, consistent with the wide array of upregulated cytokines across multiple signaling cascades. Additionally, the STZ-HFD network had the highest modularity (**Error! Reference source not found.**). Higher modularity in the STZ-HFD model indicates well-defined communities within the cytokine network, reflecting distinct functional signaling pathways in a broad inflammatory response. The lower modularity in the db/db model suggests a less distinct community structure and a more generic inflammatory response. The Jaccard index values for the STZ-HFD and WT comparisons were 0.144 (k=1) and 0.246 (k=2), indicating low similarity between these networks. Comparisons between db/db and db/+ showed slightly higher values, indicating closer similarity (**Error! Reference source not found.**). This suggests significant changes in the cytokine networks of the STZ-HFD model, while the db/db model retains more similarity to its control, reflecting less drastic alterations to the inflammatory signaling cascade.

Discussion

This study offers novel insights into the chronic inflammatory profiles and degeneration in the IVD of murine T2D models, specifically comparing the db/db and STZ-HFD mouse models. Our findings reveal critical differences between these models, underscoring the heightened relevance of the STZ-HFD model for studying T2D-related complications and inflammation in the IVD. Both db/db and STZ-HFD mice exhibit classic diabetic traits, specifically glucose intolerance and chronic hyperglycemia. These phenotypic characteristics align with established literature on human T2D (Dalgaard and Pedersen, 2001; Cefalu, 2006; Lin and Sun, 2010), validating the use of these models in diabetes research. However, while both models mimic key aspects of T2D, the STZ-HFD model parallels the etiology of human T2D

(severe insulin resistance and pancreatic beta-cell dysfunction) more closely (Gilbert et al., 2011; Stott and Marino, 2020).

In terms of IVD degeneration, our study demonstrates that STZ-HFD mice exhibit significantly more IVD degeneration compared to controls, indicating a notable degenerative phenotype. As evidenced by the structural integrity, mechanical behavior, and biochemical composition of the IVDs in these two models, the degenerative features remain primarily encapsulated by the histopathological analysis and are not further elucidated by these measures. In contrast, db/db mice, although characterized by severe obesity, insulin resistance, and chronic hyperglycemia, show less severe IVD degeneration compared to littermate controls. This fits within the broader picture of existing literature wherein db/db mice develop moderate IVD degeneration, influenced by factors such as sex and specific metabolic disruptions. Studies by Lintz et al. (2022), Natelson et al. (2020), and Li et al. (2020) support these observations, noting that while db/db mice do exhibit IVD degeneration, its typically mild or nuanced in features.

Our novel findings on the inflammatory profiles of these models serve as the strongest evidence to the superiority of the STZ-HFD model in mimicking clinically relevant T2D. The STZ-HFD model shows a significantly more robust inflammatory response, upregulating 16 different cytokines, including those associated with monocyte and macrophage recruitment, T-cell activation, and pleiotropic immune cell effects. This extensive cytokine upregulation indicates a more complex inflammatory response, which may contribute to the IVD degeneration observed in the STZ-HFD model. The relevance of these findings is underscored by literature examining the inflammatory profile of human T2D. CXCL2 is elevated in T2D patients (Rebuffat et al., 2018; Pan et al., 2021). Similarly, CCL2 and CCL3 are found at higher levels in diabetic conditions (Neumeier et al., 2011; Arner et al., 2012; Sullivan et al., 2013; Sindhu et al., 2017; Chang et al., 2021; Pan et al., 2021). The presence of CXCL9 and IL-2, aligns with findings in diabetic patients, highlighting the potential role of T-cell-mediated inflammation in the T2D IVD (Higurashi et al., 2009; Nawaz et al., 2013; Pan et al., 2021; Suri et al., 2022). CCL4 is also elevated in human studies where this cytokine are implicated in chronic inflammation in T2D (Chang et al., 2021; Pan et al., 2021; Mir et al., 2024). Moreover, the upregulation of the pleiotropic cytokine CCL5 in the STZ-HFD model, a significant marker in human T2D inflammation, further underscores the physiological relevance of this model (Keophiphath et al., 2010; Pettigrew et al., 2010; Inayat et al., 2019; Chang et al., 2021; Pan et al.,

2021; Alshammary et al., 2023; Mir et al., 2024). In summary, the STZ-HFD mouse model demonstrates a more comprehensive inflammatory response, akin to the inflammatory profile observed in human T2D, making it a more physiologically relevant model for studying diabetic inflammation in the IVD. The db/db model, while still relevant, exhibits a more limited cytokine profile. This comprehensive inflammatory characterization of the STZ-HFD model provides a valuable framework for future research into T2D-associated IVD degeneration and related pathologies.

Our network analysis further identified the STZ-HFD IVD as having a distinct inflammatory profile, revealing unique cytokine interactions and regulatory mechanisms. In the db/db model, the absence of leptin signaling results in compensatory network configurations wherein cytokines like CSF-3, CXCL-5, CXCL-9, CXCL-10, IL-4, and IL-11 are more responsible for network function. Leptin's regulatory effects on the immune system and inflammation are crucial (Francisco et al., 2018); without them, the inflammatory response to chronic stimuli from untreated T2D is stifled and incomplete. This is consistent with the db/db network, which is indicative of a constrained inflammatory response, as revealed by the short average path length and high similarity to control networks. Conversely, the STZ-HFD model, which maintains leptin signaling and mirrors human T2D etiology, exhibits extensive cytokine upregulation. As demonstrated by the cytokine network modeling, CXCL2, IL-6, IL-16, CCL11, and CSF3 are crucial mediators of this response. CXCL2, with both high centrality and significantly upregulated expression, may serve as a potential therapeutic target for inhibiting diabetic inflammation in the IVD. The presence of leptin signaling supports a more comprehensive and complex inflammatory response, reflecting the systemic impact of obesity and insulin resistance on the immune system (Francisco et al., 2018; Rebuffat et al., 2018; Sharma, 2018; Segar et al., 2019; Pan et al., 2021). The STZ-HFD network has higher modularity and longer average path length, suggesting a dispersed network with distinct functional modules. This indicates a collective of specific pathways driving the broader inflammatory response, aligning with literature above that suggests obesity and diabetes regulate a broad range of pathways.

Despite these significant findings, this study has several limitations. The selection of cytokines examined was relatively small, potentially missing other important inflammatory mediators involved in IVD degeneration. Additionally, the mechanistic link between inflammation and degeneration remains unclear and warrants further investigation. While the STZ-HFD model provides a comprehensive inflammatory

profile, the specific pathways driving the observed IVD degeneration need to be elucidated through future studies. Future directions for research based on our findings include expanding the panel of cytokines and other inflammatory mediators examined in the STZ-HFD model to gain a more complete understanding of the inflammatory landscape in T2D. Investigating the specific molecular and cellular mechanisms linking inflammation to IVD degeneration will be crucial to furthering future therapeutic approaches. Finally, exploring therapeutic interventions targeting the identified cytokine pathways could provide insights into potential treatments for T2D-related IVD degeneration.

In conclusion, our findings establish the STZ-HFD model as a more physiologically relevant model for studying T2D-related inflammation and IVD degeneration. The extensive cytokine upregulation and significant degenerative phenotype observed in this model provide a valuable framework for future research into T2D-associated pathologies. The db/db model, while still relevant, exhibits a more stunted cytokine profile and limited IVD degeneration, making it less representative of the chronic inflammatory environment seen in human T2D. These insights enhance our understanding of T2D-induced IVD degeneration and identify key cytokine pathways for therapeutic development, emphasizing the need to address these pathways holistically for effective intervention.

Conflicts of Interest

Authors declare no conflict of interest.

Acknowledgements

This work was supported by the NIH R01AR074441 and P30AR074992. Thank you to the Alafi Neuroimaging Lab for Nanozoomer Access (supported by NIH S10RR027552). Multiplex cytokine panels were performed by Eve Technologies Corp.

References

Alpantaki, K., Kampouroglou, A., Koutserimpas, C., Effraimidis, G. and Hadjipavlou, A. (2019). Diabetes mellitus as a risk factor for intervertebral disc degeneration: a critical review. *Eur. Spine J.* **28**, 2129–2144.

Alquier, T. and Poitout, V. (2018). Considerations and guidelines for mouse metabolic phenotyping in diabetes research. *Diabetologia* **61**, 526–538.

Alshammary, A. F., Alshammari, A. M., Alsobaie, S. F., Alageel, A. A. and Ali Khan, I. (2023). Evidence from genetic studies among rs2107538 variant in the *CCL5* gene and Saudi patients diagnosed with type 2 diabetes mellitus. *Saudi J. Biol. Sci.* **30**, 103658.

Al-Shukaili, A., AL-Ghafri, S., Al-Marhoobi, S., Al-Abri, S., Al-Lawati, J. and Al-Maskari, M. (2013). Analysis of Inflammatory Mediators in Type 2 Diabetes Patients. *Int. J. Endocrinol.* **2013**, 976810.

An In Vitro Organ Culture Model of the Murine Intervertebral Disc.

Arendt, L. M., McCready, J., Keller, P. J., Baker, D. D., Naber, S. P., Seewaldt, V. and Kuperwasser, C. (2013). Obesity Promotes Breast Cancer by CCL2-Mediated Macrophage Recruitment and Angiogenesis. *Cancer Res.* **73**, 6080–6093.

Arner, E., Mejhert, N., Kulyté, A., Balwierz, P. J., Pachkov, M., Cormont, M., Lorente-Cebrián, S., Ehrlund, A., Laurencikiene, J., Hedén, P., et al. (2012). Adipose Tissue MicroRNAs as Regulators of CCL2 Production in Human Obesity. *Diabetes* **61**, 1986–1993.

Atri, C., Guerfali, F. Z. and Laouini, D. (2018). Role of Human Macrophage Polarization in Inflammation during Infectious Diseases. *Int. J. Mol. Sci.* **19**, 1801.

Blondel, V. D., Guillaume, J.-L., Lambiotte, R. and Lefebvre, E. (2008). Fast unfolding of communities in large networks. *J. Stat. Mech. Theory Exp.* **2008**, P10008.

Boff, D., Crijns, H., Janssens, R., Vanheule, V., Menezes, G. B., Macari, S., Silva, T. A., Amaral, F. A. and Proost, P. (2018). The chemokine fragment CXCL9(74–103) diminishes neutrophil recruitment and joint inflammation in antigen-induced arthritis. *J. Leukoc. Biol.* **104**, 413–422.

Bond, M., Fabunmi, R. P., Baker, A. H. and Newby, A. C. (1998). Synergistic upregulation of metalloproteinase-9 by growth factors and inflammatory cytokines: an absolute requirement for transcription factor NF-κB. *FEBS Lett.* **435**, 29–34.

Boucher, J., Kleinridders, A. and Kahn, C. R. (2014). Insulin Receptor Signaling in Normal and Insulin-Resistant States. *Cold Spring Harb. Perspect. Biol.* **6**, a009191–a009191.

Broz, K., Walk, R. E. and Tang, S. Y. (2021). Complications in the spine associated with type 2 diabetes: The role of advanced glycation end-products. *Med. Nov. Technol. Devices* **11**, 100065.

Calle, M. C. and Fernandez, M. L. (2012). Inflammation and type 2 diabetes. *Diabetes Metab.* **38**, 183–191.

Cannata, F., Vadalà, G., Ambrosio, L., Fallucca, S., Napoli, N., Papalia, R., Pozzilli, P. and Denaro, V. (2019). Intervertebral disc degeneration: A focus on obesity and type 2 diabetes. *Diabetes Metab. Res. Rev.* **36**,.

Cefalu, W. T. (2006). Animal Models of Type 2 Diabetes: Clinical Presentation and Pathophysiological Relevance to the Human Condition. *ILAR J.* **47**, 186–198.

Chang, H.-D. and Radbruch, A. (2007). The Pro- and Anti-Inflammatory Potential of Interleukin-12. *Ann. N. Y. Acad. Sci.* **1109**, 40–46.

Chang, T.-T., Lin, L.-Y. and Chen, J.-W. (2021). A Novel Resolution of Diabetes: C-C Chemokine Motif Ligand 4 Is a Common Target in Different Types of Diabetes by Protecting Pancreatic Islet Cell and Modulating Inflammation. *Front. Immunol.* **12**,.

Chen, H., Charlat, O., Tartaglia, L. A., Woolf, E. A., Weng, X., Ellis, S. J., Lakey, N. D., Culpepper, J., More, K. J., Breitbart, R. E., et al. (1996). Evidence That the Diabetes Gene Encodes the Leptin Receptor: Identification of a Mutation in the Leptin Receptor Gene in db/db Mice. *Cell* **84**, 491–495.

Chen, L., Deng, H., Cui, H., Fang, J., Zuo, Z., Deng, J., Li, Y., Wang, X. and Zhao, L. (2017). Inflammatory responses and inflammation-associated diseases in organs. *Oncotarget* **9**, 7204–7218.

Chen, L., Zhang, Q., Yu, C., Wang, F. and Kong, X. (2020). Functional roles of CCL5/RANTES in liver disease. *Liver Res.* **4**, 28–34.

Curic, G. (2021). Intervertebral Disc and Adipokine Leptin—Loves Me, Loves Me Not. *Int. J. Mol. Sci.* **22**, 375.

Dalgaard, L. T. and Pedersen, O. (2001). Uncoupling proteins: functional characteristics and role in the pathogenesis of obesity and Type II diabetes. *Diabetologia* **44**, 946–965.

Daryabor, G., Atashzar, M. R., Kabelitz, D., Meri, S. and Kalantar, K. (2020). The Effects of Type 2 Diabetes Mellitus on Organ Metabolism and the Immune System. *Front. Immunol.* **11**,.

de Candia, P., Prattichizzo, F., Garavelli, S., De Rosa, V., Galgani, M., Di Rella, F., Spagnuolo, M. I., Colamatteo, A., Fusco, C., Micillo, T., et al. (2019). Type 2 Diabetes: How Much of an Autoimmune Disease? *Front. Endocrinol.* **10**,.

De Geer, C. M. (2018). Cytokine Involvement in Biological Inflammation Related to Degenerative Disorders of the Intervertebral Disk: A Narrative Review. *J. Chiropr. Med.* **17**, 54–62.

DeLeon-Pennell, K. Y., Iyer, R. P., Ero, O. K., Cates, C. A., Flynn, E. R., Cannon, P. L., Jung, M., Shannon, D., Garrett, M. R., Buchanan, W., et al. Periodontal-induced chronic inflammation triggers macrophage secretion of Ccl12 to inhibit fibroblast-mediated cardiac wound healing. *JCI Insight* **2**, e94207.

Eckhardt, B. A., Rowsey, J. L., Thicke, B. S., Fraser, D. G., O'Grady, K. L., Bondar, O. P., Hines, J. M., Singh, R. J., Thoreson, A. R., Rakshit, K., et al. Accelerated osteocyte senescence and skeletal fragility in mice with type 2 diabetes. *JCI Insight* **5**, e135236.

Etna, M. P., Giacomini, E., Severa, M. and Coccia, E. M. (2014). Pro- and anti-inflammatory cytokines in tuberculosis: A two-edged sword in TB pathogenesis. *Semin. Immunol.* **26**, 543–551.

Francisco, V., Pino, J., Campos-Cabaleiro, V., Ruiz-Fernández, C., Mera, A., Gonzalez-Gay, M. A., Gómez, R. and Gualillo, O. (2018). Obesity, Fat Mass and Immune System: Role for Leptin. *Front. Physiol.* **9**, 640.

Gilbert, E. R., Fu, Z. and Liu, D. (2011). Development of a Nongenetic Mouse Model of Type 2 Diabetes. *J. Diabetes Res.* **2011**, 416254.

Gruber, H. E., Ingram, J. A., Hoelscher, G. L. and Hanley, E. N. (2007). Leptin expression by annulus cells in the human intervertebral disc. *Spine J.* **7**, 437–443.

Guest, C. B., Park, M. J., Johnson, D. R. and Freund, G. G. (2008). The implication of proinflammatory cytokines in type 2 diabetes. *Front. Biosci.-Landmark* **13**, 5187–5194.

Han, Y.-C., Ma, B., Guo, S., Yang, M., Li, L.-J., Wang, S.-J. and Tan, J. (2018). Leptin regulates disc cartilage endplate degeneration and ossification through activation of the MAPK-ERK signalling pathway in vivo and in vitro. *J. Cell. Mol. Med.* **22**, 2098–2109.

He, M., Dong, H., Huang, Y., Lu, S., Zhang, S., Qian, Y. and Jin, W. (2016). Astrocyte-Derived CCL2 is Associated with M1 Activation and Recruitment of Cultured Microglial Cells. *Cell. Physiol. Biochem.* **38**, 859–870.

Herder, C., Carstensen, M. and Ouwens, D. M. (2013). Anti-inflammatory cytokines and risk of type 2 diabetes. *Diabetes Obes. Metab.* **15**, 39–50.

Higurashi, M., Ohya, Y., Joh, K., Muraguchi, M., Nishimura, M., Terawaki, H., Yagui, K., Hashimoto, N., Saito, Y. and Yamada, K. (2009). Increased urinary levels of CXCL5, CXCL8 and CXCL9 in patients with Type 2 diabetic nephropathy. *J. Diabetes Complications* **23**, 178–184.

House, I. G., Savas, P., Lai, J., Chen, A. X. Y., Oliver, A. J., Teo, Z. L., Todd, K. L., Henderson, M. A., Giuffrida, L., Petley, E. V., et al. (2020). Macrophage-Derived CXCL9 and CXCL10 Are Required for Antitumor Immune Responses Following Immune Checkpoint Blockade. *Clin. Cancer Res.* **26**, 487–504.

Huang, J., Yang, G., Xiong, X., Wang, M., Yuan, J., Zhang, Q., Gong, C., Qiu, Z., Meng, Z., Xu, R., et al. (2020). Age-related CCL12 Aggravates Intracerebral Hemorrhage-induced Brain Injury via Recruitment of Macrophages and T Lymphocytes. *Aging Dis.* **11**, 1103–1115.

Inayat, H., Azim, M. K. and Baloch, A. A. (2019). Analysis of Inflammatory Gene Expression Profile of Peripheral Blood Leukocytes in Type 2 Diabetes. *Immunol. Invest.* **48**, 618–631.

Islam, Md. S. and Wilson, R. D. (2012). Experimentally Induced Rodent Models of Type 2 Diabetes. In *Animal Models in Diabetes Research* (ed. Joost, H.-G.), Al-Hasani, H.), and Schürmann, A.), pp. 161–174. Totowa, NJ: Humana Press.

Itariu, B. K. and Stulnig, T. M. (2014). Autoimmune Aspects of Type 2 Diabetes Mellitus - A Mini-Review. *Gerontology* **60**, 189–196.

Jhawar, B. S., Fuchs, C. S., Colditz, G. A. and Stampfer, M. J. (2006). Cardiovascular risk factors for physician-diagnosed lumbar disc herniation. *Spine J.* **6**, 684–691.

Juhas, U., Ryba-Stanisławowska, M., Szargiej, P. and Myśliwska, J. (2015). Different pathways of macrophage activation and polarization. *Postępy Hig. Med. Dośw.* **69**, 496–502.

Keophiphath, M., Rouault, C., Divoux, A., Clément, K. and Lacasa, D. (2010). CCL5 Promotes Macrophage Recruitment and Survival in Human Adipose Tissue. *Arterioscler. Thromb. Vasc. Biol.* **30**, 39–45.

Kranjc, M. K., Novak, M., Pestell, R. G. and Lah, T. T. (2019). Cytokine CCL5 and receptor CCR5 axis in glioblastoma multiforme. *Radiol. Oncol.* **53**, 397–406.

Kuo, P., Tuong, Z. K., Teoh, S. M., Frazer, I. H., Mattarollo, S. R. and Leggatt, G. R. (2018). HPV16E7-Induced Hyperplasia Promotes CXCL9/10 Expression and Induces CXCR3+ T-Cell Migration to Skin. *J. Invest. Dermatol.* **138**, 1348–1359.

Kusakabe, T., Tanioka, H., Ebihara, K., Hirata, M., Miyamoto, L., Miyanaga, F., Hige, H., Aotani, D., Fujisawa, T., Masuzaki, H., et al. (2009). Beneficial effects of leptin on glycaemic and lipid control in a mouse model of type 2 diabetes with increased adiposity induced by streptozotocin and a high-fat diet. *Diabetologia* **52**, 675–683.

Lança, T., Costa, M. F., Gonçalves-Sousa, N., Rei, M., Grosso, A. R., Penido, C. and Silva-Santos, B. (2013). Protective Role of the Inflammatory CCR2/CCL2 Chemokine Pathway through Recruitment of Type 1 Cytotoxic γδ T Lymphocytes to Tumor Beds. *J. Immunol.* **190**, 6673–6680.

Lee, G.-H., Proenca, R., Montez, J. M., Carroll, K. M., Darvishzadeh, J. G., Lee, J. I. and Friedman, J. M. (1996). Abnormal splicing of the leptin receptor in diabetic mice. *Nature* **379**, 632–635.

Li, Z., Shen, J., Wu, W. K. K., Yu, X., Liang, J., Qiu, G. and Liu, J. (2013). The role of leptin on the organization and expression of cytoskeleton elements in nucleus pulposus cells. *J. Orthop. Res.* **31**, 847–857.

Li, X., Liu, X., Wang, Y., Cao, F., Chen, Z., Hu, Z., Yu, B., Feng, H., Ba, Z., Liu, T., et al. (2020). Intervertebral disc degeneration in mice with type II diabetes induced by leptin receptor deficiency. *BMC Musculoskelet. Disord.* **21**, 77.

Lim, S. Y., Yuzhalin, A. E., Gordon-Weeks, A. N. and Muschel, R. J. (2016). Targeting the CCL2-CCR2 signaling axis in cancer metastasis. *Oncotarget* **7**, 28697–28710.

Lin, Y. and Sun, Z. (2010). Current views on type 2 diabetes. *J. Endocrinol.* **204**, 1.

Lin, K. H. and Tang, S. Y. (2017). The Quantitative Structural and Compositional Analyses of Degenerating Intervertebral Discs Using Magnetic Resonance Imaging and Contrast-Enhanced Micro-Computed Tomography. *Ann. Biomed. Eng.* **45**, 2626–2634.

Lin, K. H., Wu, Q., Leib, D. J. and Tang, S. Y. (2016). A novel technique for the contrast-enhanced microCT imaging of murine intervertebral discs. *J. Mech. Behav. Biomed. Mater.* **63**, 66–74.

Lintz, M., Walk, R. E., Tang, S. Y. and Bonassar, L. J. (2022). The degenerative impact of hyperglycemia on the structure and mechanics of developing murine intervertebral discs. *JOR Spine* **5**, e1191.

Liu, J. W., Abraham, A. C. and Y. Tang, S. (2015). The high-throughput phenotyping of the viscoelastic behavior of whole mouse intervertebral discs using a novel method of dynamic mechanical testing. *J. Biomech.* **48**, 2189–2194.

Liu, X., Pan, F., Ba, Z., Wang, S. and Wu, D. (2018). The potential effect of type 2 diabetes mellitus on lumbar disc degeneration: a retrospective single-center study. *J. Orthop. Surg.* **13**, 52.

Luo, J., Quan, J., Tsai, J., Hobensack, C. K., Sullivan, C., Hector, R. and Reaven, G. M. (1998). Nongenetic mouse models of non—insulin-dependent diabetes mellitus. *Metabolism* **47**, 663–668.

Lyu, F.-J., Cui, H., Pan, H., MC Cheung, K., Cao, X., Iatridis, J. C. and Zheng, Z. (2021). Painful intervertebral disc degeneration and inflammation: from laboratory evidence to clinical interventions. *Bone Res.* **9**, 1–14.

Malemud, C. J. (2019). Inhibition of MMPs and ADAM/ADAMTS. *Biochem. Pharmacol.* **165**, 33–40.

Marcovecchio, P. M., Thomas, G. and Salek-Ardakani, S. (2021). CXCL9-expressing tumor-associated macrophages: new players in the fight against cancer. *J. Immunother. Cancer* **9**, e002045.

Markovics, A., Rosenthal, K. S., Mikecz, K., Carambula, R. E., Ciemielewski, J. C. and Zimmerman, D. H. (2022). Restoring the Balance between Pro-Inflammatory and Anti-Inflammatory Cytokines in the Treatment of Rheumatoid Arthritis: New Insights from Animal Models. *Biomedicines* **10**, 44.

Medrikova, D., Jilkova, Z. M., Bardova, K., Janovska, P., Rossmeisl, M. and Kopecky, J. (2012). Sex differences during the course of diet-induced obesity in mice: adipose tissue expandability and glycemic control. *Int. J. Obes.* **36**, 262–272.

Melgoza, I. P., Chenna, S. S., Tessier, S., Zhang, Y., Tang, S. Y., Ohnishi, T., Novais, E. J., Kerr, G. J., Mohanty, S., Tam, V., et al. (2021). Development of a standardized histopathology scoring

system using machine learning algorithms for intervertebral disc degeneration in the mouse model—An ORS spine section initiative. *JOR SPINE* **4**, e1164.

Mir, M. M., Alfaifi, J., Sohail, S. K., Rizvi, S. F., Akhtar, M. T., Alghamdi, M. A. A., Mir, R., Wani, J. I., Sabah, Z. U., Alhumaydhi, F. A., et al. (2024). The Role of Pro-Inflammatory Chemokines CCL-1, 2, 4, and 5 in the Etiopathogenesis of Type 2 Diabetes Mellitus in Subjects from the Asir Region of Saudi Arabia: Correlation with Different Degrees of Obesity. *J. Pers. Med.* **14**, 743.

Molinos, M., Almeida, C. R., Caldeira, J., Cunha, C., Gonçalves, R. M. and Barbosa, M. A. (2015). Inflammation in intervertebral disc degeneration and regeneration. *J. R. Soc. Interface* **12**, 20141191.

Mortara, L., Balza, E., Bruno, A., Poggi, A., Orecchia, P. and Carnemolla, B. (2018). Anti-cancer Therapies Employing IL-2 Cytokine Tumor Targeting: Contribution of Innate, Adaptive and Immunosuppressive Cells in the Anti-tumor Efficacy. *Front. Immunol.* **9**,.

Motwani, M. and Gilroy, D. (2015). Macrophage development and polarization in chronic inflammation. *Semin. Immunol.* **27**,.

Mu, J., Woods, J., Zhou, Y.-P., Roy, R. S., Li, Z., Zycband, E., Feng, Y., Zhu, L., Li, C., Howard, A. D., et al. (2006). Chronic Inhibition of Dipeptidyl Peptidase-4 With a Sitagliptin Analog Preserves Pancreatic β-Cell Mass and Function in a Rodent Model of Type 2 Diabetes. *Diabetes* **55**, 1695–1704.

Mu, J., Petrov, A., Eiermann, G. J., Woods, J., Zhou, Y.-P., Li, Z., Zycband, E., Feng, Y., Zhu, L., Roy, R. S., et al. (2009). Inhibition of DPP-4 with sitagliptin improves glycemic control and restores islet cell mass and function in a rodent model of type 2 diabetes. *Eur. J. Pharmacol.* **623**, 148–154.

Natelson, D. M., Lai, A., Krishnamoorthy, D., Hoy, R. C., Iatridis, J. C. and Illien-Jünger, S. (2020). Leptin signaling and the intervertebral disc: Sex dependent effects of leptin receptor deficiency and Western diet on the spine in a type 2 diabetes mouse model. *PLOS ONE* **15**, e0227527.

National Diabetes Statistics Report | Diabetes | CDC (2022).

Navone, S. E., Marfia, G., Giannoni, A., Beretta, M., Guarnaccia, L., Gualtierotti, R., Nicoli, D., Rampini, P. and Campanella, R. (2017). Inflammatory mediators and signalling pathways controlling intervertebral disc degeneration. *Histol. Histopathol.* 523–542.

Nawaz, M. I., Van Raemdonck, K., Mohammad, G., Kangave, D., Van Damme, J., Abu El-Asrar, A. M. and Struyf, S. (2013). Autocrine CCL2, CXCL4, CXCL9 and CXCL10 signal in retinal endothelial cells and are enhanced in diabetic retinopathy. *Exp. Eye Res.* **109**, 67–76.

Neumeier, M., Bauer, S., Brühl, H., Eisinger, K., Kopp, A., Abke, S., Walter, R., Schäffler, A. and Buechler, C. (2011). Adiponectin stimulates release of CCL2, -3, -4 and -5 while the surface abundance of CCR2 and -5 is simultaneously reduced in primary human monocytes. *Cytokine* **56**, 573–580.

Ochiai, E., Sa, Q., Brogli, M., Kudo, T., Wang, X., Dubey, J. P. and Suzuki, Y. (2015). CXCL9 Is Important for Recruiting Immune T Cells into the Brain and Inducing an Accumulation of the T Cells to the Areas of Tachyzoite Proliferation to Prevent Reactivation of Chronic Cerebral Infection with *Toxoplasma gondii*. *Am. J. Pathol.* **185**, 314–324.

Pan, X., Kaminga, A. C., Wen, S. W. and Liu, A. (2021). Chemokines in Prediabetes and Type 2 Diabetes: A Meta-Analysis. *Front. Immunol.* **12**,.

650 **Pelisch, N., Rosas Almanza, J., Stehlik, K. E., Aperi, B. V. and Kroner, A.** (2020). CCL3 contributes to
651 secondary damage after spinal cord injury. *J. Neuroinflammation* **17**, 362.

652 **Petersen, M. C. and Shulman, G. I.** (2018). Mechanisms of Insulin Action and Insulin Resistance.
653 *Physiol. Rev.* **98**, 2133–2223.

654 **Pettersson, U. S., Waldén, T. B., Carlsson, P.-O., Jansson, L. and Phillipson, M.** (2012). Female Mice
655 are Protected against High-Fat Diet Induced Metabolic Syndrome and Increase the Regulatory T
656 Cell Population in Adipose Tissue. *PLOS ONE* **7**, e46057.

657 **Pettigrew, K. A., McKnight, A. J., Patterson, C. C., Kilner, J., Sadlier, D. M. and Maxwell, A. P.** (2010).
658 Resequencing of the CCL5 and CCR5 genes and investigation of variants for association with
659 diabetic nephropathy. *J. Hum. Genet.* **55**, 248–251.

660 **Pinto, E. M., Neves, J. R., Laranjeira, M. and Reis, J.** (2023). The importance of inflammatory
661 biomarkers in non-specific acute and chronic low back pain: a systematic review. *Eur. Spine J.*

662 **Rebuffat, S. A., Sidot, E., Guzman, C., Azay-Milhau, J., Jover, B., Lajoix, A.-D. and Peraldi-Roux, S.**
663 (2018). Adipose tissue derived-factors impaired pancreatic β-cell function in diabetes. *Biochim.*
664 *Biophys. Acta BBA - Mol. Basis Dis.* **1864**, 3378–3387.

665 **Risbud, M. V. and Shapiro, Irving. M.** (2014). Role of Cytokines in Intervertebral Disc Degeneration:
666 Pain and Disc-content. *Nat. Rev. Rheumatol.* **10**, 44–56.

667 **Robinson, D., Mirovsky, Y., Halperin, N., Evron, Z. and Nevo, Z.** (1998). Changes in Proteoglycans of
668 Intervertebral Disc in Diabetic Patients: A Possible Cause of Increased Back Pain. *Spine* **23**, 849.

669 **Ruytinx, P., Proost, P., Van Damme, J. and Struyf, S.** (2018). Chemokine-Induced Macrophage
670 Polarization in Inflammatory Conditions. *Front. Immunol.* **9**,.

671 **Sagar, D., Lamontagne, A., Foss, C. A., Khan, Z. K., Pomper, M. G. and Jain, P.** (2012). Dendritic cell
672 CNS recruitment correlates with disease severity in EAE via CCL2 chemotaxis at the blood–brain
673 barrier through paracellular transmigration and ERK activation. *J. Neuroinflammation* **9**, 245.

674 **Sakaguchi, K., Takeda, K., Maeda, M., Ogawa, W., Sato, T., Okada, S., Ohnishi, Y., Nakajima, H. and**
675 **Kashiwagi, A.** (2015). Glucose area under the curve during oral glucose tolerance test as an
676 index of glucose intolerance. *Diabetol. Int.* **7**, 53–58.

677 **Sakellaridis, N.** (2006). The influence of diabetes mellitus on lumbar intervertebral disk herniation. *Surg.*
678 *Neurol.* **66**, 152–154.

679 **Segar, A. H., Fairbank, J. C. T. and Urban, J.** (2019). Leptin and the intervertebral disc: a biochemical
680 link exists between obesity, intervertebral disc degeneration and low back pain—an in vitro study
681 in a bovine model. *Eur. Spine J.* **28**, 214–223.

682 **Shachar, I. and Karin, N.** (2013). The dual roles of inflammatory cytokines and chemokines in the
683 regulation of autoimmune diseases and their clinical implications. *J. Leukoc. Biol.* **93**, 51–61.

684 **Shamji, M. F., Setton, L. A., Jarvis, W., So, S., Chen, J., Jing, L., Bullock, R., Isaacs, R. E., Brown, C.**
685 **and Richardson, W. J.** (2010). Proinflammatory cytokine expression profile in degenerated and
686 herniated human intervertebral disc tissues. *Arthritis Rheum.* **62**, 1974–1982.

687 **Sharma, A.** (2018). The Role of Adipokines in Intervertebral Disc Degeneration. *Med. Sci.* **6**, 34.

Sheng, D., Ma, W., Zhang, R., Zhou, L., Deng, Q., Tu, J., Chen, W., Zhang, F., Gao, N., Dong, M., et al. (2022). Ccl3 enhances docetaxel chemosensitivity in breast cancer by triggering proinflammatory macrophage polarization. *J. Immunother. Cancer* **10**, e003793.

Sindhu, S., Akhter, N., Arefanian, H., Al-Roub, A. A., Ali, S., Wilson, A., Al-Hubail, A., Al-Beloushi, S., Al-Zanki, S. and Ahmad, R. (2017). Increased circulatory levels of fractalkine (CX3CL1) are associated with inflammatory chemokines and cytokines in individuals with type-2 diabetes. *J. Diabetes Metab. Disord.* **16**, 15.

Sindhu, S., Kochumon, S., Shenouda, S., Wilson, A., Al-Mulla, F. and Ahmad, R. (2019). The Cooperative Induction of CCL4 in Human Monocytic Cells by TNF-α and Palmitate Requires MyD88 and Involves MAPK/NF-κB Signaling Pathways. *Int. J. Mol. Sci.* **20**, 4658.

Srinivasan, K. and Ramarao, P. (2007). Animal models in type 2 diabetes research: An overview. *Indian J. Med. Res.* **125**, 451.

Stott, N. L. and Marino, J. S. (2020). High Fat Rodent Models of Type 2 Diabetes: From Rodent to Human. *Nutrients* **12**, 3650.

Stubbins, R. E., Holcomb, V. B., Hong, J. and Núñez, N. P. (2012). Estrogen modulates abdominal adiposity and protects female mice from obesity and impaired glucose tolerance. *Eur. J. Nutr.* **51**, 861–870.

Sullivan, T. J., Miao, Z., Zhao, B. N., Ertl, L. S., Wang, Y., Krasinski, A., Walters, M. J., Powers, J. P., Dairaghi, D. J., Baumgart, T., et al. (2013). Experimental evidence for the use of CCR2 antagonists in the treatment of type 2 diabetes. *Metabolism* **62**, 1623–1632.

Suri, S., Mitra, P., Abhilasha, A., Saxena, I., Garg, M. K., Bohra, G. K. and Sharma, P. (2022). Role of interleukin-2 and interleukin-18 in newly diagnosed type 2 diabetes mellitus. *J. Basic Clin. Physiol. Pharmacol.* **33**, 185–190.

Tian, Y., Yuan, W., Fujita, N., Wang, J., Wang, H., Shapiro, I. M. and Risbud, M. V. (2013). Inflammatory Cytokines Associated with Degenerative Disc Disease Control Aggrecanase-1 (ADAMTS-4) Expression in Nucleus Pulposus Cells through MAPK and NF-κB. *Am. J. Pathol.* **182**, 2310–2321.

Velikova, T. V., Kabakchieva, P. P., Assyov, Y. S. and Georgiev, T. A. (2021). Targeting Inflammatory Cytokines to Improve Type 2 Diabetes Control. *BioMed Res. Int.* **2021**, 1–12.

Venetz, D., Ponzoni, M., Schiraldi, M., Ferreri, A. J. M., Bertoni, F., Doglioni, C. and Uguccioni, M. (2010). Perivascular expression of CXCL9 and CXCL12 in primary central nervous system lymphoma: T-cell infiltration and positioning of malignant B cells. *Int. J. Cancer* **127**, 2300–2312.

Wang, B., P., C. C. and Pippin, J. J. (2014). Leptin- and Leptin Receptor-Deficient Rodent Models: Relevance for Human Type 2 Diabetes. *Curr. Diabetes Rev.* **10**, 131–145.

Wuertz, K. and Haglund, L. (2013). Inflammatory Mediators in Intervertebral Disk Degeneration and Discogenic Pain. *Glob. Spine J.* **3**, 175–184.

Xu, P., Zhang, F., Chang, M., Zhong, C., Sun, C.-H., Zhu, H.-R., Yao, J.-C., Li, Z.-Z., Li, S.-T., Zhang, W.-C., et al. (2021a). Recruitment of γδ T cells to the lesion via the CCL2/CCR2 signaling after spinal cord injury. *J. Neuroinflammation* **18**, 64.

Figure 1. Experimental design, animal model, and workflow of the current study. (A) The db/db model arises due to a point mutation in the leptin receptor gene, while the STZ-HFD model develops diabetes through a pro-glycemic diet and beta cell impairment. Both models present symptoms of obesity, chronic hyperglycemia, and insulin resistance, though the magnitude can vary both between and within each model. **(B)** The experimental timeline outlines the progression of the study for both models. The db/db mice are acquired at skeletal maturity (12 weeks old) and sacrificed after metabolic measurements are collected. For the STZ-HFD model, mice undergo a lead-in phase of 4-6 weeks on a HFD followed by a single low dose of STZ. Subsequently, the experimental phase for the STZ-HFD mice continues with HFD for 12 weeks, with periodic assessments of fasting blood glucose, A1c levels, and glucose tolerance. **(C)** After sacrifice, FSUs, consisting of the intervertebral disc and the adjacent vertebral bodies, are extracted from mice. FSUs are then utilized for terminal measures pictured above.

Xu, L., Chen, Y., Nagashimada, M., Ni, Y., Zhuge, F., Chen, G., Li, H., Pan, T., Yamashita, T., Mukaida, N., et al. (2021b). CC chemokine ligand 3 deficiency ameliorates diet-induced steatohepatitis by regulating liver macrophage recruitment and M1/M2 status in mice. *Metabolism* **125**, 154914.

Yang, J., Agarwal, M., Ling, S., Teitz-Tennenbaum, S., Zemans, R. L., Osterholzer, J. J., Sisson, T. H. and Kim, K. K. (2020). Diverse Injury Pathways Induce Alveolar Epithelial Cell CCL2/12, Which Promotes Lung Fibrosis. *Am. J. Respir. Cell Mol. Biol.* **62**, 622–632.

Yin, R., Xue, Y., Hu, J., Hu, X. and Shen, Q. (2020). The effects of diet and streptozotocin on metabolism and gut microbiota in a type 2 diabetes mellitus mouse model. *Food Agric. Immunol.* **31**, 723–739.

Zeng, Z., Lan, T., Wei, Y. and Wei, X. (2022). CCL5/CCR5 axis in human diseases and related treatments. *Genes Dis.* **9**, 12–27.

Zhang, Y., Lin, J. and Wei, F. (2015). The Function and Roles of ADAMTS-7 in Inflammatory Diseases. *Mediators Inflamm.* **2015**, 801546.

Zhang, X., Fan, L., Wu, J., Xu, H., Leung, W. Y., Fu, K., Wu, J., Liu, K., Man, K., Yang, X., et al. (2019). Macrophage p38α promotes nutritional steatohepatitis through M1 polarization. *J. Hepatol.* **71**, 163–174.

Figure 4. Comparative analysis of IVD structure, mechanics, and composition are similar between db/db and STZ-HFD mice. (A)-(C) NPVF, NIDI, and DHI indicate few significant differences in structural integrity between the models. **(D)-(F)** Load slope, energy dissipated, and phase shift demonstrating no significant variations in viscoelastic mechanical behavior. **(G)-(I)** Biochemical content measurements, including collagen, s-GAG, and AGEs, show no significant differences.

Figure 2. Both db/db and STZ-HFD mice represent a characteristically T2D phenotype. (A) AUC GTT shows elevated glucose

Figure 5. STZ-HFD IVD Produces a More Pro-Inflammatory Microenvironment than the db/db IVD in Comparative Analysis of Cytokine Expression. (A) The STZ-HFD model shows a significantly higher fold increase for eight cytokines: CXCL2, CCL2, CCL3, CCL4, CCL12 (monocyte/macrophage associated), IL-2, CXCL9 (T-cell associated), and CCL5 (pleiotropic). **(B)** The STZ-HFD model encompasses a broader and more pronounced cytokine response compared to the db/db model, highlighting the extensive upregulation of inflammatory cytokines in the STZ-HFD model.

Figure 3. STZ-HFD mice exhibit more severe histopathological IVD degeneration compared to db/db mice. (A) Comparison

Figure 6. STZ-HFD IVD Invokes Unique Inflammatory Signaling Pathways in Networks of Cytokine Expression. (A) The STZ-HFD model shows a distinct network structure, demonstrating the unique upregulation of various inflammatory pathways **(B)** The STZ-HFD and db/db networks each rely on a number of unique (red/blue) and shared (purple) cytokines, indicating both leptin-dependent and leptin-independent inflammatory signaling cascades **(C)** The STZ-HFD mouse model displays a fragmented and modular cytokine network, indicating the parallel signaling of multiple signaling pathways.

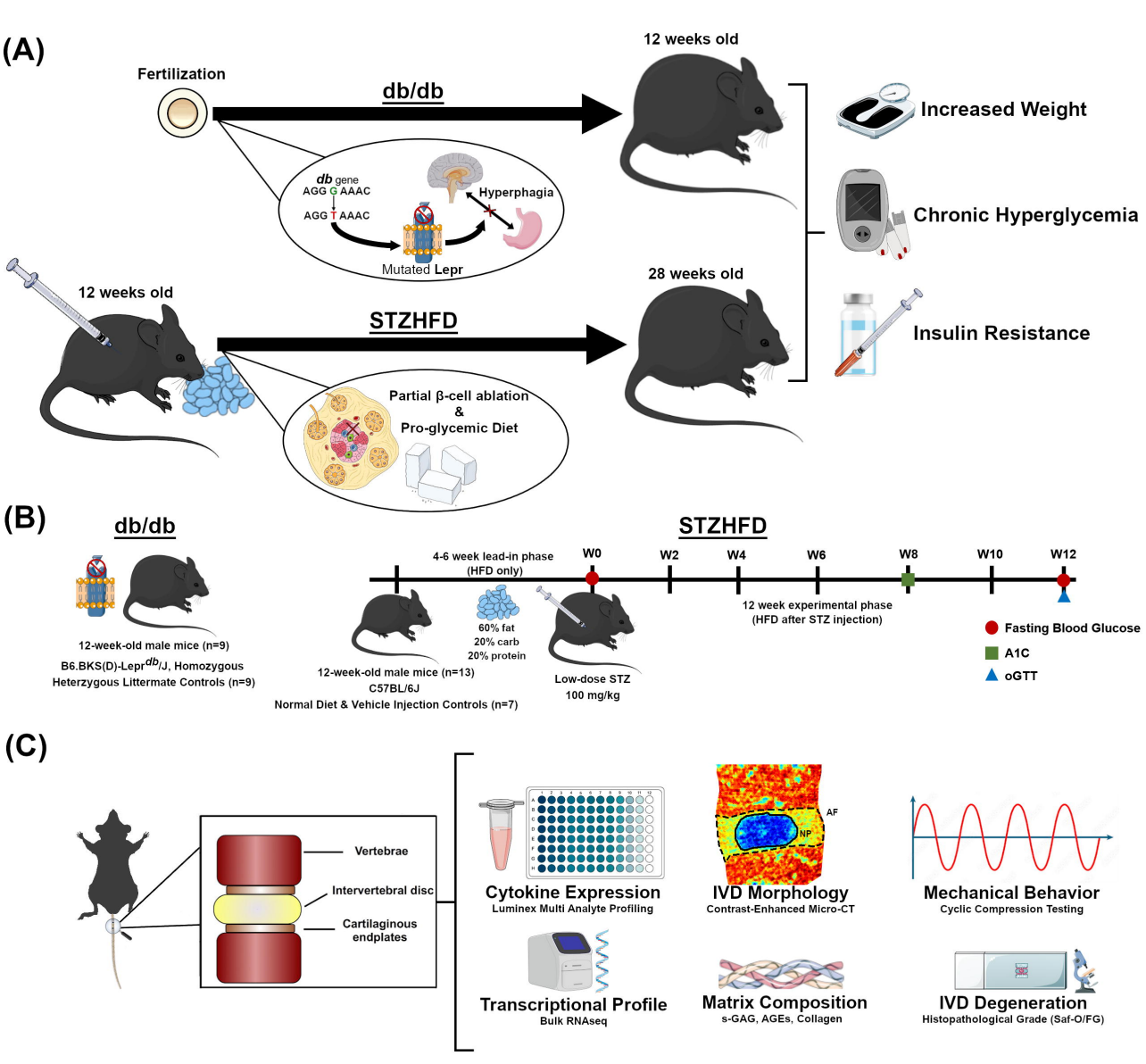
(A)
Fertilization
db/db
12 weeks old
db gene
AGG G AAAC
AGG T AAAC
Hyperphagia
Mutated Lepr
Increased Weight
Chronic Hyperglycemia
Insulin Resistance
12 weeks old
STZHFD
28 weeks old
Partial β-cell ablation
&
Pro-glycemic Diet
(B)
db/db
12-week-old male mice (n=9)
B6.BKS(D)-Leprdb/J, Homozygous
Heterzygous Littermate Controls (n=9)
STZHFD
4-6 week lead-in phase
(HFD only)
W0
W2
W4
W6
W8
W10
W12
60% fat
20% carb
20% protein
12-week-old male mice (n=13)
C57BL/6J
Normal Diet & Vehicle Injection Controls (n=7)
Low-dose STZ
100 mg/kg
12 week experimental phase
(HFD after STZ injection)
Fasting Blood Glucose
A1C
oGTT
(C)
Vertebrae
Intervertebral disc
Cartilaginous
endplates
Cytokine Expression
Luminex Multi Analyte Profiling
AF
NP
IVD Morphology
Contrast-Enhanced Micro-CT
Mechanical Behavior
Cyclic Compression Testing
Transcriptional Profile
Bulk RNAseq
Matrix Composition
s-GAG, AGEs, Collagen
IVD Degeneration
Histopathological Grade (Saf-O/FG)

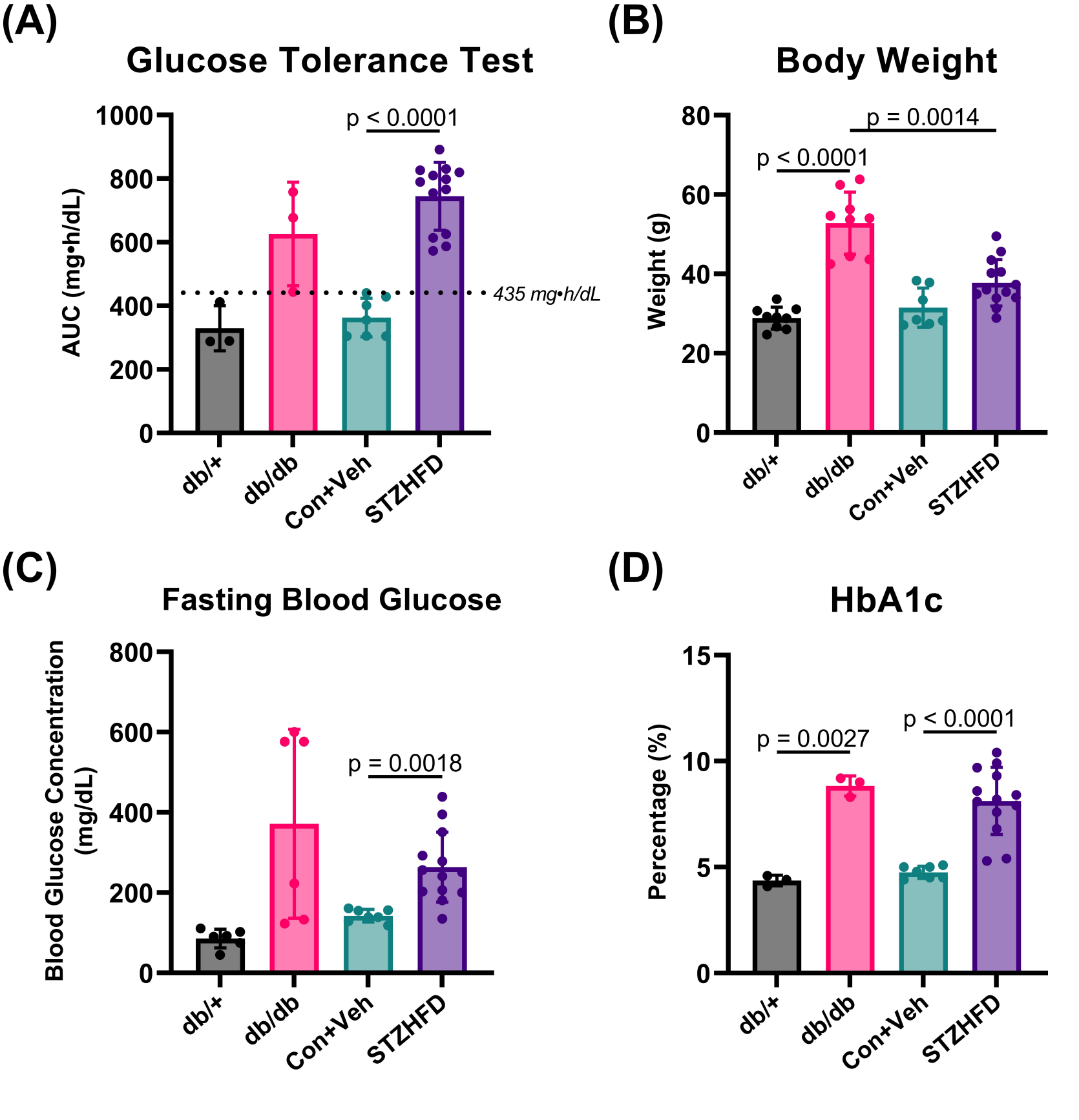
(A)
Glucose Tolerance Test
AUC (mg•h/dL)
1000
800
600
400
200
0
p < 0.0001
435 mg•h/dL
db/+
db/db
Con+Veh
STZHFD
(B)
Body Weight
Weight (g)
80
60
40
20
0
p = 0.0014
p < 0.0001
db/+
db/db
Con+Veh
STZHFD
(C)
Fasting Blood Glucose
Blood Glucose Concentration (mg/dL)
800
600
400
200
0
p = 0.0018
db/+
db/db
Con+Veh
STZHFD
(D)
HbA1c
Percentage (%)
15
10
5
0
p = 0.0027
p < 0.0001
db/+
db/db
Con+Veh
STZHFD

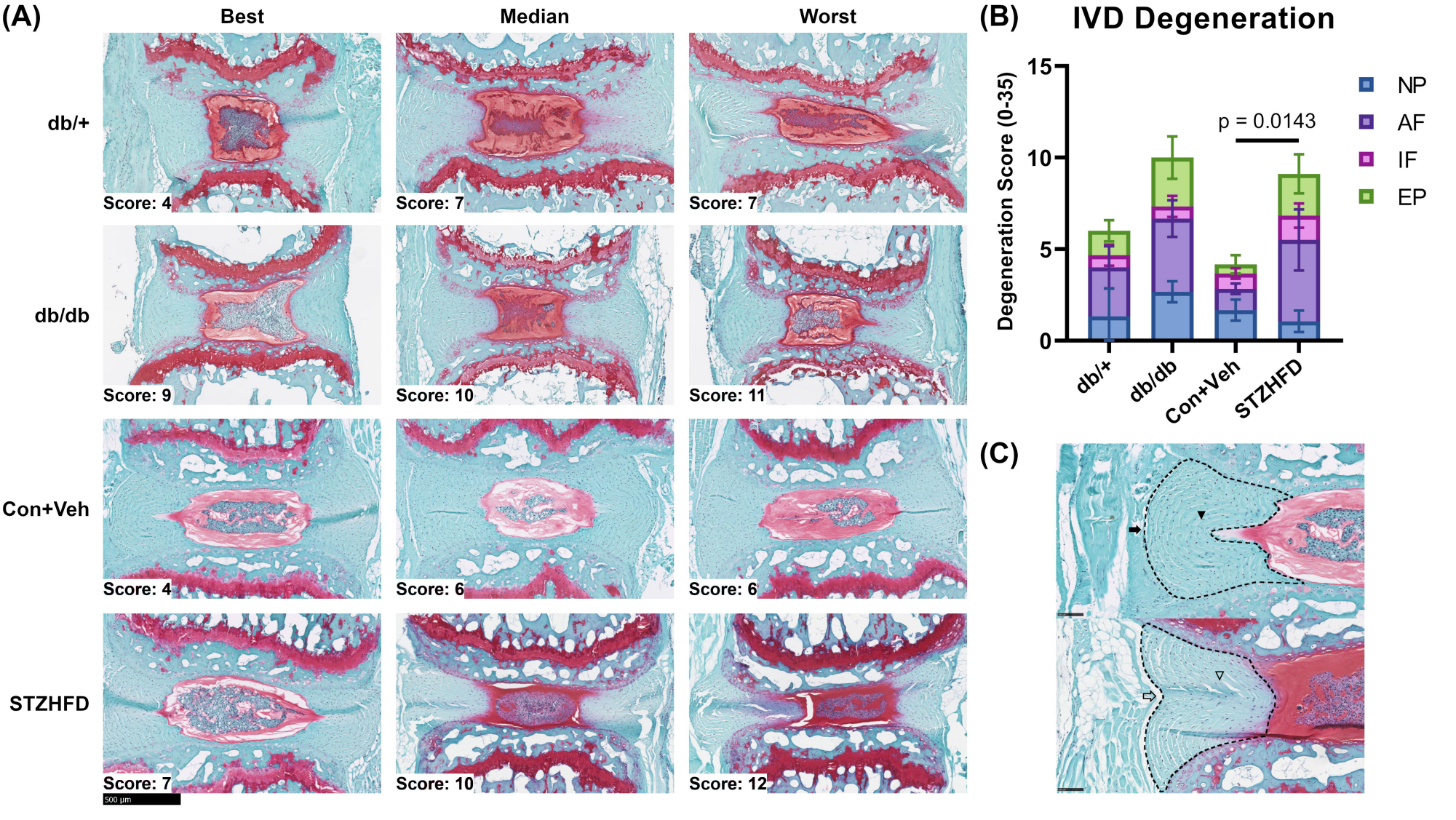
(A)
Best
Median
Worst
db/+
db/db
Con+Veh
STZHFD
Score: 4
Score: 7
Score: 7
Score: 9
Score: 10
Score: 11
Score: 4
Score: 6
Score: 6
Score: 7
Score: 10
Score: 12
500 µm
(B)
IVD Degeneration
Degeneration Score (0-35)
15
10
5
0
p = 0.0143
NP
AF
IF
EP
db/+
db/db
Con+Veh
STZHFD
(C)

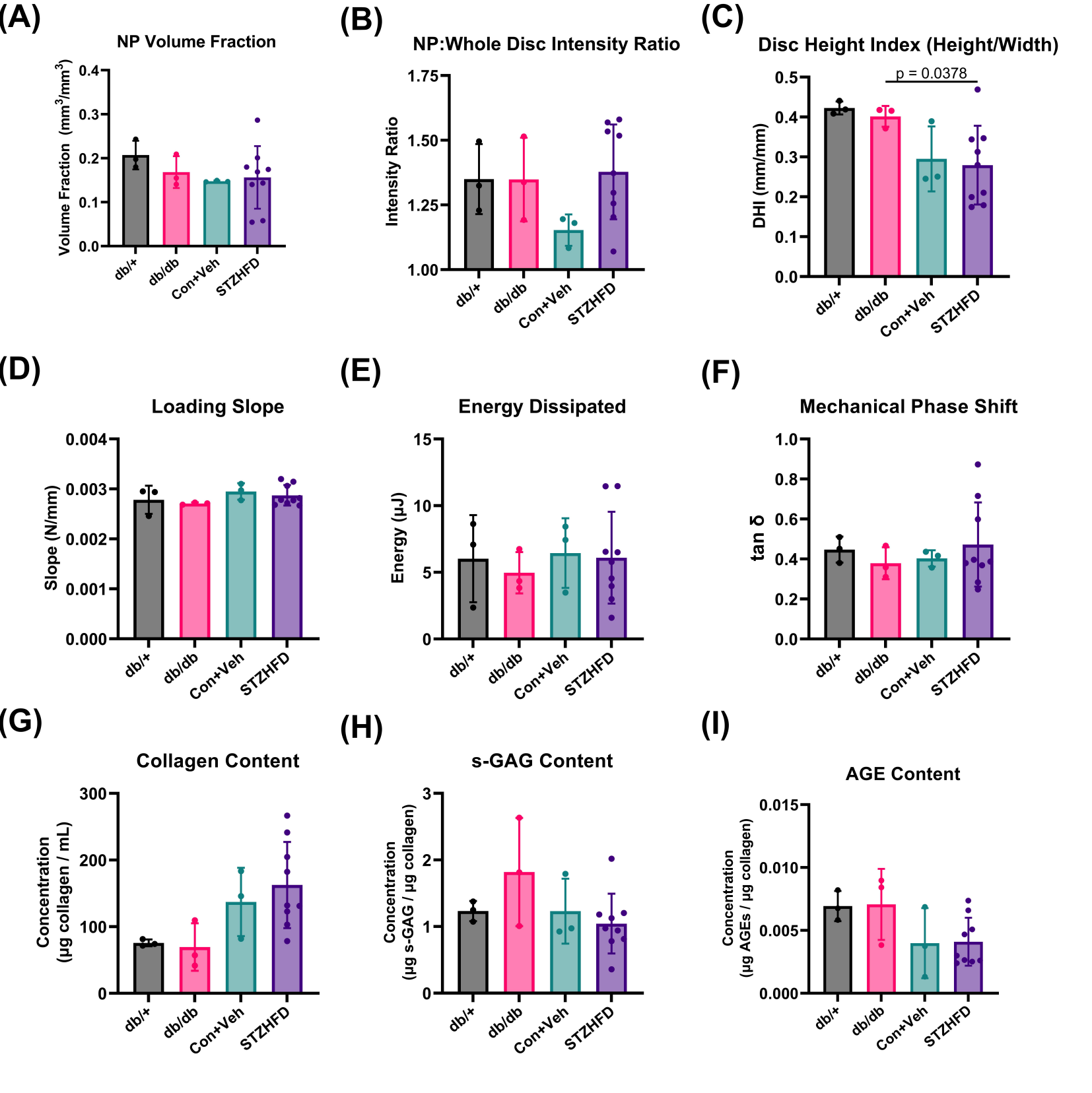
(A)
NP Volume Fraction
Volume Fraction (mm3/mm3)
0.4
0.3
0.2
0.1
0.0
db/+
db/db
Con+Veh
STZHFD
(B)
NP:Whole Disc Intensity Ratio
Intensity Ratio
1.75
1.50
1.25
1.00
db/+
db/db
Con+Veh
STZHFD
(C)
Disc Height Index (Height/Width)
p = 0.0378
DHI (mm/mm)
0.5
0.4
0.3
0.2
0.1
0.0
db/+
db/db
Con+Veh
STZHFD
(D)
Loading Slope
Slope (N/mm)
0.004
0.003
0.002
0.001
0.000
db/+
db/db
Con+Veh
STZHFD
(E)
Energy Dissipated
Energy (µJ)
15
10
5
0
db/+
db/db
Con+Veh
STZHFD
(F)
Mechanical Phase Shift
tan δ
1.0
0.8
0.6
0.4
0.2
0.0
db/+
db/db
Con+Veh
STZHFD
(G)
Collagen Content
Concentration (µg collagen / mL)
300
200
100
0
db/+
db/db
Con+Veh
STZHFD
(H)
s-GAG Content
Concentration (µg s-GAG / µg collagen)
3
2
1
0
db/+
db/db
Con+Veh
STZHFD
(I)
AGE Content
Concentration (µg AGEs / µg collagen)
0.015
0.010
0.005
0.000
db/+
db/db
Con+Veh
STZHFD

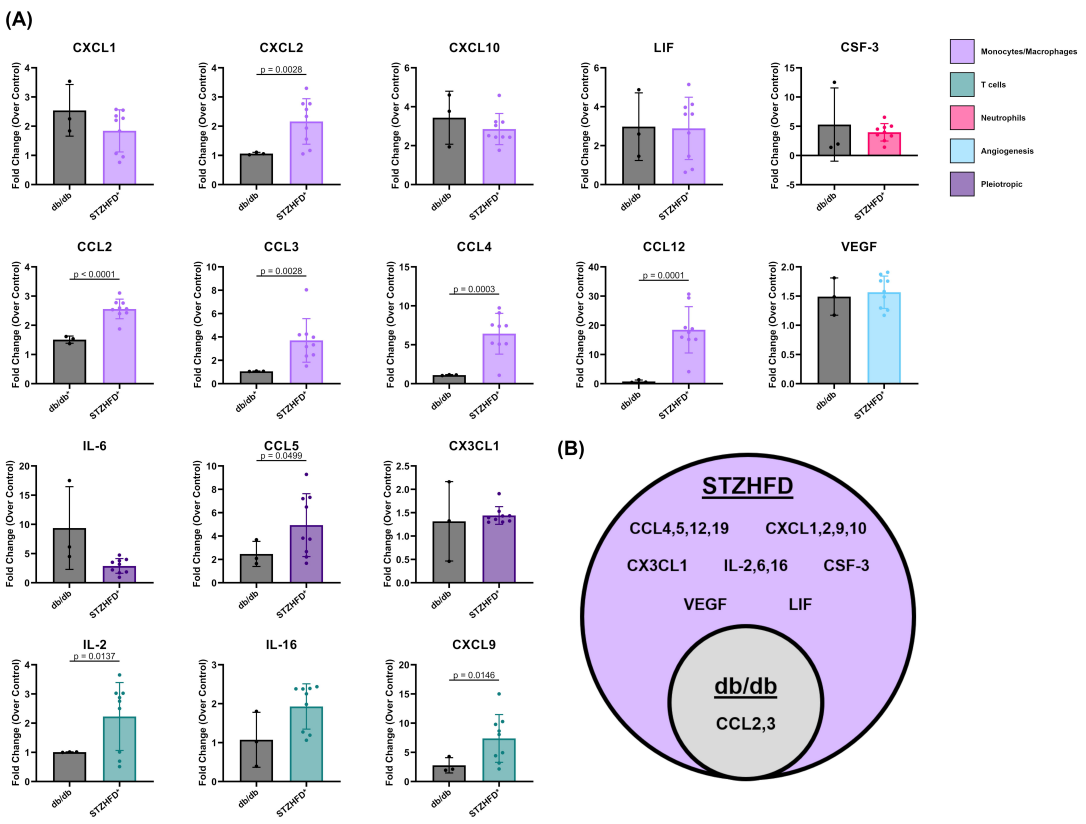
(A)
CXCL1
CXCL2
p = 0.0028
CXCL10
LIF
CSF-3
CCL2
p < 0.0001
CCL3
p = 0.0028
CCL4
p = 0.0003
CCL12
p = 0.0001
VEGF
IL-6
CCL5
p = 0.0499
CX3CL1
IL-2
p = 0.0137
IL-16
CXCL9
p = 0.0146
Fold Change (Over Control)
db/db
STZHFD
Monocytes/Macrophages
T cells
Neutrophils
Angiogenesis
Pleiotropic
(B)
STZHFD
CCL4,5,12,19
CXCL1,2,9,10
CX3CL1
IL-2,6,16
CSF-3
VEGF
LIF
db/db
CCL2,3

(A)

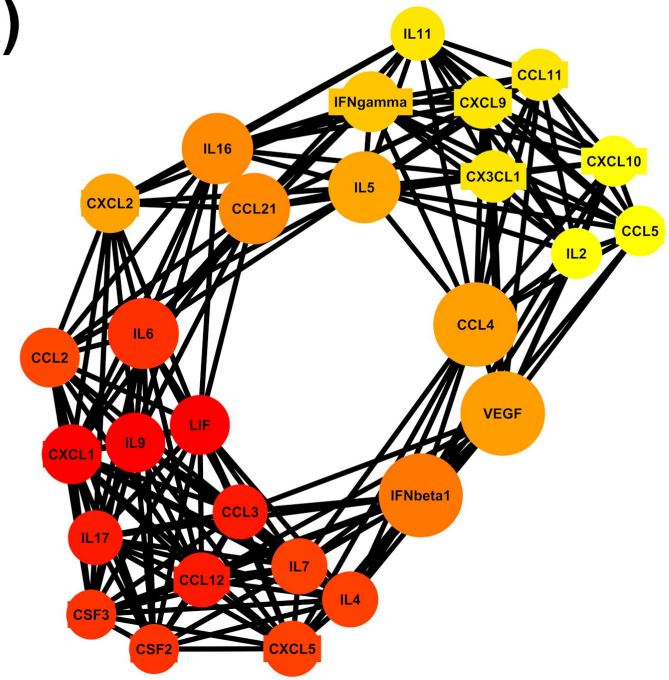

Control+Vehicle

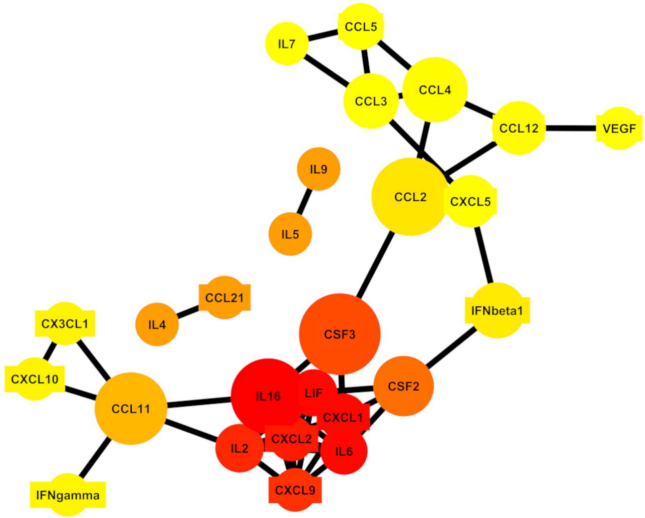

STZHFD

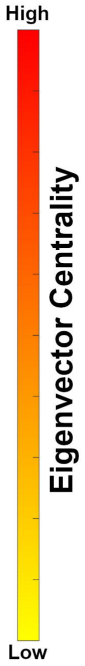

(B)

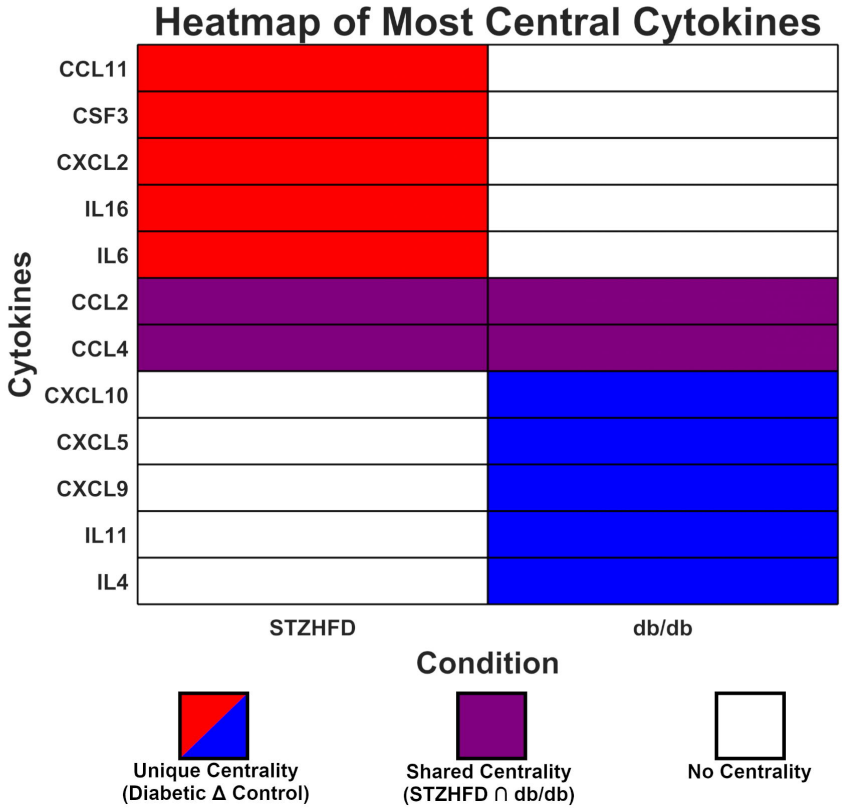

(C)

Metric	Con+Veh	STZHFD	db/+	db/db
Path Length	1.3	2.3	1.3	1.3
Modularity	0.34	0.45	0.29	0.18
	Con+Veh vs STZHFD	db/db vs STZHFD	db/+ vs db/db	db/+ vs Con+Veh
Jaccard Index (k=1)	0.14	0.13	0.21	0.15
Jaccard Index (k=2)	0.25	0.24	0.37	0.32